Genetic and cellular analyses of zebrafish atrioventricular cushion and valve development

Dimitris Beis[1,*,§], Thomas Bartman[1,†], Suk-Won Jin[1], Ian C. Scott[1], Leonard A. D'Amico[1], Elke A. Ober[1,‡], Heather Verkade[1], Julie Frantsve[1], Holly A. Field[1], Ann Wehman[2], Herwig Baier[2], Alexandra Tallafuss[3], Laure Bally-Cuif[3], Jau-Nian Chen[4], Didier Y. R. Stainier[1,¶] and Benno Jungblut[1,§]

[1]Department of Biochemistry and Biophysics and Cardiovascular Research Institute, University of California, San Francisco, San Francisco, CA 94143, USA
[2]Department of Physiology, University of California, San Francisco, San Francisco, CA 94143, USA
[3]Zebrafish Neurogenetics Group, IDG, GSF-National Research Center for Environment and Health, Ingolstaedter Landstrasse 1, 85764 Neuherberg, Germany
[4]Department of Molecular, Cellular, and Developmental Biology, University of California Los Angeles, CA 90095, USA
*Present address: Foundation for Biomedical Research of the Academy of Athens, Basic Research Center, Athens, Greece
†Present address: Divisions of Neonatology, Pulmonary Biology and Developmental Biology Cincinnati Children's Hospital Medical Center, OH 45229, USA
‡Present address: National Institute for Medical Research, Division of Developmental Biology, Mill Hill, London NW7 1AA, UK
§These authors contributed equally to this work
¶Author for correspondence (didier_stainier@biochem.ucsf.edu)

Accepted 7 July 2005

Development 132, 4193-4204
Published by The Company of Biologists 2005
doi:10.1242/dev.01970

Summary

Defects in cardiac valve morphogenesis and septation of the heart chambers constitute some of the most common human congenital abnormalities. Some of these defects originate from errors in atrioventricular (AV) endocardial cushion development. Although this process is being extensively studied in mouse and chick, the zebrafish system presents several advantages over these models, including the ability to carry out forward genetic screens and study vertebrate gene function at the single cell level. In this paper, we analyze the cellular and subcellular architecture of the zebrafish heart during stages of AV cushion and valve development and gain an unprecedented level of resolution into this process. We find that endocardial cells in the AV canal differentiate morphologically before the onset of epithelial to mesenchymal transformation, thereby defining a previously unappreciated step during AV valve formation. We use a combination of novel transgenic lines and fluorescent immunohistochemistry to analyze further the role of various genetic (Notch and Calcineurin signaling) and epigenetic (heart function) pathways in this process. In addition, from a large-scale forward genetic screen we identified 55 mutants, defining 48 different genes, that exhibit defects in discrete stages of AV cushion development. This collection of mutants provides a unique set of tools to further our understanding of the genetic basis of cell behavior and differentiation during AV valve development.

Key words: Heart, AV canal, Endocardium, Notch, Calcineurin, Zebrafish

Introduction

Understanding how cardiac valves develop is of fundamental importance to both developmental biologists and clinicians. Cardiac valves form during the late steps of heart morphogenesis and function throughout the life of the animal to prevent retrograde blood flow. Hemodynamic influences and a large number of signaling pathways converge to generate a functional heart, and tight spatial and temporal control of these signals is vital for normal organogenesis, including valve development (reviewed by Armstrong and Bischoff, 2004; Olson, 2004). Consistent with the complexity of the process, congenital heart disease (CHD) is the most common type of congenital anomaly. One to two percent of live births have some form of CHD with defects in valve and septa formation being the most common subtype (Hoffman and Kaplan, 2002). Numerous mouse models that exhibit structural and functional anomalies resembling human CHD have been generated, thereby elucidating the role of an increasing number of signaling pathways in heart development (reviewed by Gruber and Epstein, 2004).

The mammalian heart has four chambers: two atria, separated by an interatrial septum; and two ventricles separated by an interventricular septum. At the AV junction lie two valves: the tricuspid valve, with three leaflets separating the right atrium and ventricle; and a bicuspid mitral valve separating the left-sided chambers. These cardiac valves derive from endocardial cushions (ECs), transient structures that form from the cellularization and expansion of the extracellular matrix (ECM) between the endocardium and myocardium at the AV canal. In an initial step of cushion formation, endocardial cells at the AV canal undergo an epithelial to mesenchymal transformation (EMT), delaminate and invade the ECM. Studies on chick and mouse cushion development, which were aimed at identifying molecules regulating EMT,

Development

Development

have predominantly used an in vitro system of explanted cushion tissue on a type I collagen gel (Bernanke and Markwald, 1982). Using this system, Krug et al. (Krug et al., 1987) showed that myocardial cells from the AV boundary, but not those from the ventricle, induce endocardial cells to undergo EMT. Likewise, only endocardial cells from the AV canal, but not those from the ventricle, can undergo EMT in response to a myocardial signal (Runyan and Markwald, 1983). Therefore, the endocardial and myocardial cells at the AV canal appear to have unique properties in comparison to other myocardial cells (reviewed by Eisenberg and Markwald, 1995).

One key pathway in the interactions between myocardial and endocardial cells at the AV canal appears to be Calcineurin/NFAT signaling (Chang et al., 2004; de la Pompa et al., 1998; Ranger et al., 1998). *vegf* expression is suppressed in the AV canal myocardial cells as a direct target of the NFATc 2/3/4 transcription factors, thereby permitting the adjacent endocardial cells to undergo EMT. At a later stage, endocardial calcineurin function through NFATc1 is required for valve morphogenesis (Chang et al., 2004).

In addition to *NFATc/calcineurin* and *Vegf*, a number of other genes have been implicated in the formation of the valves and septa. For example, mutations in the transcription factor genes *NKX25*, *GATA4* and *TBX5* have been found in individuals with atrial septal defects (Basson et al., 1997; Garg et al., 2003; Schott et al., 1998). It has also recently been described that E9.5 mouse embryos carrying mutations in either *Notch1* or the Notch transcriptional effector gene *RBPJk* exhibit a collapse of the endocardium and lack mesenchymal cushion cells, indicative of a failure in EMT (Timmerman et al., 2004). These phenotypes suggest that Notch signaling is required to regulate the morphological changes associated with the progression of differentiation of the endocardium. However, it remains unclear at what stage the differentiation of the endocardium fails in these mutants and how endocardial cell disorganization leads to chamber collapse.

Studies carried out in zebrafish have identified additional signaling pathways involved in valve morphogenesis. Zebrafish mutants in the tumor suppressor adenomatous polyposis coli (*apc*) gene exhibit a profuse endocardial layer at the AV boundary and form excessive ECs at 72 hours post-fertilization (hpf) as a result of a constitutively active Wnt/β-catenin signaling pathway (Hurlstone et al., 2003). Other studies have demonstrated that pathways implicated in valve development in mammals also regulate this process in zebrafish. For example, blocking Calcineurin signaling by cyclosporine A (CsA) treatment causes EC phenotypes in zebrafish embryos (Chang et al., 2004), although the cellular effects of CsA treatment on cushion and valve formation remain to be analyzed.

The zebrafish heart consists of two chambers: an atrium and a ventricle. Rhythmic contractions start at 22 hpf and looping occurs near 36 hpf. Although the first morphological differences between the two cardiac chambers can be observed after the formation of the linear heart tube, molecular differences between atrium and ventricle are apparent much earlier (reviewed by Yelon and Stainier, 1999). The AV canal forms at the border between the atrium and ventricle and the first molecular indication of AV canal specification in zebrafish occurs at ~37 hpf with the restriction of *bmp4* and *versican* expression to the AV myocardium (Walsh and Stainier, 2001). At ~45 hpf, the expression of *notch1b* becomes restricted to the AV endocardium (Westin and Lardelli, 1997). The differentiated AV canal suffices to prevent retrograde blood flow in the 48 hpf zebrafish heart as mutants with defects in AV canal differentiation display blood regurgitation. One such mutant is *jekyll*, which was shown to carry a mutation in *ugdh* (Walsh and Stainier, 2001), a homologue of *Drosophila Sugarless* (Hacker et al., 1997). The restriction of *bmp4*, *versican* and *notch1b* expression, as well as the upregulation of *Tg(Tie2:EGFP)*^{s849} (Stainier et al., 2002), all of which mark the specification of the AV canal, fail to occur in *jek* mutant embryos (Walsh and Stainier, 2001), indicating that *jek/ugdh* is required upstream of AV canal specification. A similar failure in the upregulation of *Tg(Tie2:EGFP)*^{s849} at the AV canal is observed in *silent heart* (*sih*) mutant embryos (Bartman et al., 2004). *sih* corresponds to the *cardiac troponin T* gene and homozygous mutant hearts do not contract (Sehnert et al., 2002). These and other results (Bartman et al., 2004) suggest that mechanical stimuli caused by the beating heart are essential for AV canal differentiation. Similarly, hemodynamic shear stress has been implicated in zebrafish valve development (Hove et al., 2003).

The zebrafish system offers a unique combination of advantages for studying cell biology during vertebrate organogenesis, as zebrafish embryos develop externally and are practically transparent throughout development, thereby allowing non-invasive observation. Especially advantageous to the study of cardiovascular development is the fact that the embryos, because of their small size, receive sufficient oxygen by passive diffusion alone to allow heart morphogenesis to proceed to a late stage, even in the total absence of circulation (Stainier, 2001). Furthermore, the amenability to forward and reverse genetics enables the identification of novel signaling pathways that regulate a developmental process, as well as the further analysis of previously identified genes. In the first forward genetic screen for heart mutations in Boston, a series of mutants displaying blood regurgitation between the atrium and ventricle were identified (Stainier et al., 1996), but unfortunately few were successfully propagated or preserved.

In this paper, we present a detailed description of the cellular events underlying AV canal differentiation, EC formation and morphogenesis of cushions into valve leaflets. We find that AV canal endocardial cells differentiate by adopting a cuboidal shape before the onset of EC formation. We use several novel transgenic lines and immunohistochemical markers to analyze further the role of Notch and calcineurin function, as well as mechanical stimuli in AV canal differentiation. We also introduce a large set of mutants that exhibit defects in discrete stages of AV cushion development.

Materials and methods

Zebrafish strains and lines

Zebrafish were raised under standard laboratory conditions at 28°C (Westerfield, 2000). We used the following transgenic lines: *Tg(Tie2:EGFP)*^{s849} (Motoike et al., 2000), *Tg(0.7her5:EGFP)*^{ne2067} (Tallafuss and Bally-Cuif, 2003) and *Tg(UAS:myc-Notch1a-intra)*^{kca3} (Scheer, 1999). We generated the *Tg(flk1:EGFP)*^{s843} and *Tg(flk1:Gal4-UAS:EGFP)*^{s848} constructs by cloning a 7 kb fragment of the *flk1* promoter (ending at base –3 of the transcriptional start site, PubMed id AF487829) upstream of promoter-less EGFP and GAL4-

UAS:EGFP (Koster and Fraser, 2001) constructs, respectively. We injected 200 pg of linearized DNA without the plasmid backbone into one cell-stage embryos and selected individual transgenic carrier adults by screening for fluorescent progeny. In total, six carriers were recovered for the *Tg(flk1:EGFP)*^{s843} line and four for the *Tg(flk1:Gal4-UAS:EGFP)*^{s848} (with essentially identical expression patterns and levels).

Immunohistochemistry and confocal microscopy

We used the following antibodies at the indicated dilutions: mouse monoclonal antibodies zn5 and zn8 (Zebrafish stock center and Hybridoma Bank) at 1:10, mouse anti β-catenin (BD Biosciences) at 1:200 (Hurlstone et al., 2003), rabbit anti-Myc (Sigma) at 1:200, rabbit anti-fibronectin (Sigma) at 1:200 (Trinh and Stainier, 2004) and mouse IgG anti ZO-1 (Zymed) at 1:200 (Trinh et al., 2005).

Embryos were fixed for 2 hours at room temperature with 4% (zn5, anti β-catenin, anti-Myc, anti-fibronectin) or 2% PFA (anti ZO-1). Whole-mount antibody staining was carried out in PBT (4% BSA, 0.3% Triton and 0.02% NaN3 in PBS pH 7.3). Stained embryos were embedded in NuSieve GTG low melting agarose and cut into 200 μm sections with a Leica VT1000S vibratome. Sections were incubated ON with rhodamine phalloidin (Molecular Probes) 1:50 in PBDT (PBS, 0.1% Tween, 1% DMSO) for filamentous actin staining and with topro3 (Molecular Probes; 1:5000 in PBDT) for nuclear staining. Images were acquired using a Zeiss LSM5 Pascal confocal microscope.

Pharmacological treatment

A 10 mM stock of DAPT (Calbiochem) in DMSO was diluted in embryo water. Embryos were dechorionated and incubated in 10 or 100 μM DAPT in embryo water. Control embryos were incubated in 1% DMSO in embryo water. Embryos were fixed, immunostained and imaged. A 50 mg/ml stock of CsA in ethanol was diluted in embryo water to a final concentration of 10 μg/ml. Embryos were incubated within their chorions and then were fixed, immunostained and imaged. Control embryos were incubated in 0.02% ethanol. Similar results were obtained for concentrations of CsA ranging from 5 to 50 μg/ml.

ENU mutagenesis and screen

We screened approximately 9076 F3 clutches from 2392 ENU-mutagenized F2 families that were generated in the context of two different screens (Wehman et al., 2005) (E.A.O., H.V., H.A.F., Duc Dong, Pia Aanstad, Takuya Sakaguchi, Michel Bagnat, Chantilly Munson, Won-Suk Chung, Chong Shin, Silvia Curado, Ryan Anderson, J.F., D.B., T.B. and D.Y.R.S., unpublished). Based on the number of crosses per F2 family, we calculate that our screen surveyed 2723 genomes. The specific locus test for each screen indicated a mutation rate of approximately 0.3% per gene per genome.

Results

In order to understand the genetic control of cell behavior during the development of the AV valve, we analyzed cellular events starting from the looped heart tube stage until the adult heart stage.

AV canal differentiation

To visualize endocardial cells, we used the *Tg(Tie2:EGFP)*^{s849} (Motoike et al., 2000) and *Tg(flk1:EGFP)*^{s843} lines, both of which express GFP in all endothelial cells. We counterstained all samples with rhodamine phalloidin, which outlines all

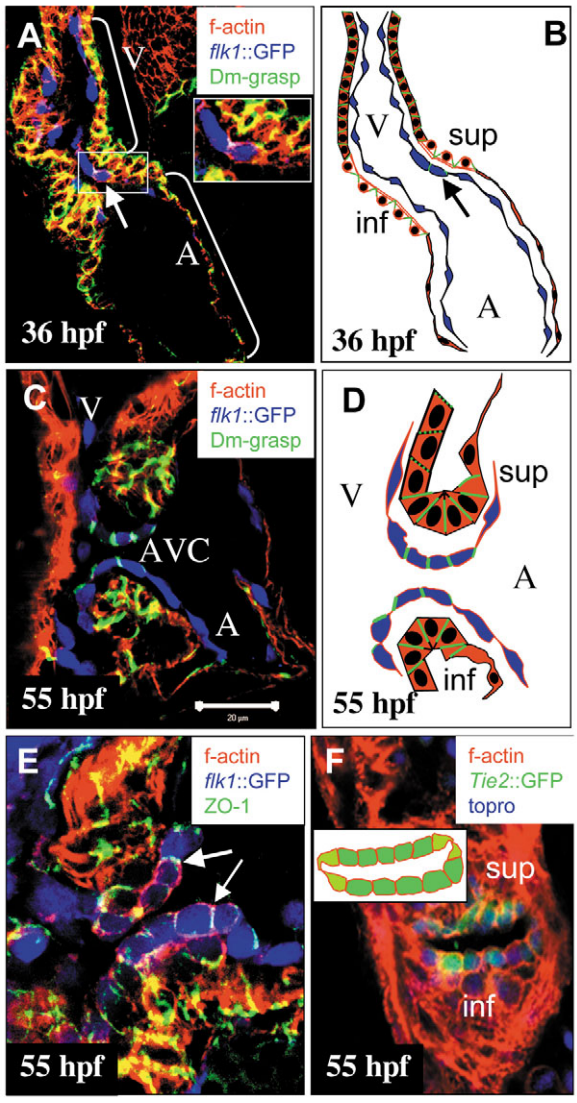

Fig. 1. Cellular differentiation of wild-type AV canal between 36 and 55 hpf. Confocal images of the heart at 36 hpf (A) and the AV canal at 55 hpf (C,E,F). (A,C,E) *Tg(flk1:EGFP)*^{s843} (pseudo-colored blue) embryos stained with rhodamine phalloidin (red) and immunostained for Dm-grasp (pseudo-colored green) (A,C) or for ZO-1 (pseudo-colored green) (E). (F) *Tg(Tie2:EGFP)*^{s849} (green) embryo stained with topro (blue) and rhodamine phalloidin (red). (A) At 36 hpf, the heart has looped and the endocardium (in blue) is single layered and squamous. Arrow indicates one endocardial cell expressing Dm-grasp. (B) Schematic representation of the heart shown in A. (C) At 55 hpf, the AV canal endocardial cells exhibit a cuboidal shape and Dm-grasp is localized laterally. Ventricular and atrial endocardial cells appear squamous and devoid of Dm-grasp expression. Myocardial cells in the superior (sup) and inferior (inf) ECFR of the AV canal exhibit stronger expression of laterally localized Dm-grasp compared with ventricular and atrial myocardial cells. (D) Schematic representation of the AV canal shown in C. (E) ZO-1 is expressed by all myocardial and endocardial cells, including the cuboidal endocardial cells lining the AV canal. Arrows indicate ZO-1 localized in tight junctions between two neighboring cuboidal endocardial cells. (F) Transverse section. A five or six cell-wide sheet of cuboidal cells line the superior and inferior regions of the AV canal. Laterally and in this plane, two squamous cells (hinge cells; light green) connect the sheets of cuboidal cells. The inset is a schematic representation of the pattern of endocardial cell shapes across the AV canal. A, atrium; V, ventricle; AVC, atrioventricular canal; inf, inferior ECFR; sup: superior ECFR.

cardiac cells and strongly stains the sarcomeric actin of the myocardial cells. In addition, we used the zn5 monoclonal antibody to visualize cell-cell borders in the embryonic myocardium. This antibody recognizes Dm-grasp, a cell-surface adhesion molecule of the immunoglobulin superfamily (Fashena and Westerfield, 1999), that we find localized to the lateral side of myocardial cells and differentiated AV canal endocardial cells.

At 36 hpf, the zebrafish embryonic heart tube has looped, placing the ventricle to the right and the atrium to the left of the midline (Fig. 1A). Endocardial cells are squamous throughout the heart, except for a single cell at the border between the atrium and ventricle, which has a cuboidal shape and has initiated Dm-grasp expression (Fig. 1A,B arrow). This shape change and initiation of Dm-grasp expression are the earliest manifestations of endocardial differentiation in the AV canal.

Over the next 12 hours, endocardial and myocardial cells located in the AV canal further differentiate morphologically. At 55 hpf, myocardial cells at the AV boundary show stronger staining for Dm-grasp than neighboring atrial or ventricular cells (Fig. 1C,D). Endocardial cells lining the AV canal form a single layer of cuboidal cells that express Dm-grasp laterally in contrast to the squamous Dm-grasp negative endocardial cells lining the heart chambers (Fig. 1C,D). These data establish Dm-grasp as a reliable marker for differentiated AV canal endocardial cells. In addition, this cuboidal shape of AV endocardial cells has not been described before during chick or mouse EC formation, where the earliest reported cellular event is an epithelial to mesenchymal transformation. In order to confirm that cuboidal endocardial cells retain their epithelial organization, we stained 55 hpf embryos for ZO1, a molecule associated with tight junctions in epithelial cells. Fig. 1E shows that both squamous and cuboidal endocardial cells express ZO-1, while rhodamine phalloidin staining is upregulated around the basolateral extent of the cuboidal AV canal endocardial cells. A similar distribution of β-catenin in these cells (data not shown) indicates the presence of adherens junctions and further supports the claim that cuboidal AV endocardial cells retain an epithelial organization.

The morphological differentiation of the AV canal described here indicates that this region represents a developmental segment (or field) in which cells have differentiated relative to their neighbors. Consequently, the AV canal forms two boundaries: one with the ventricle and another with the atrium. Consistent with mouse (Webb et al., 1998) and avian (Yan and Sinning, 2001) nomenclature, we refer to the region of the AV canal adjacent to the inner curvature of the ventricle as the

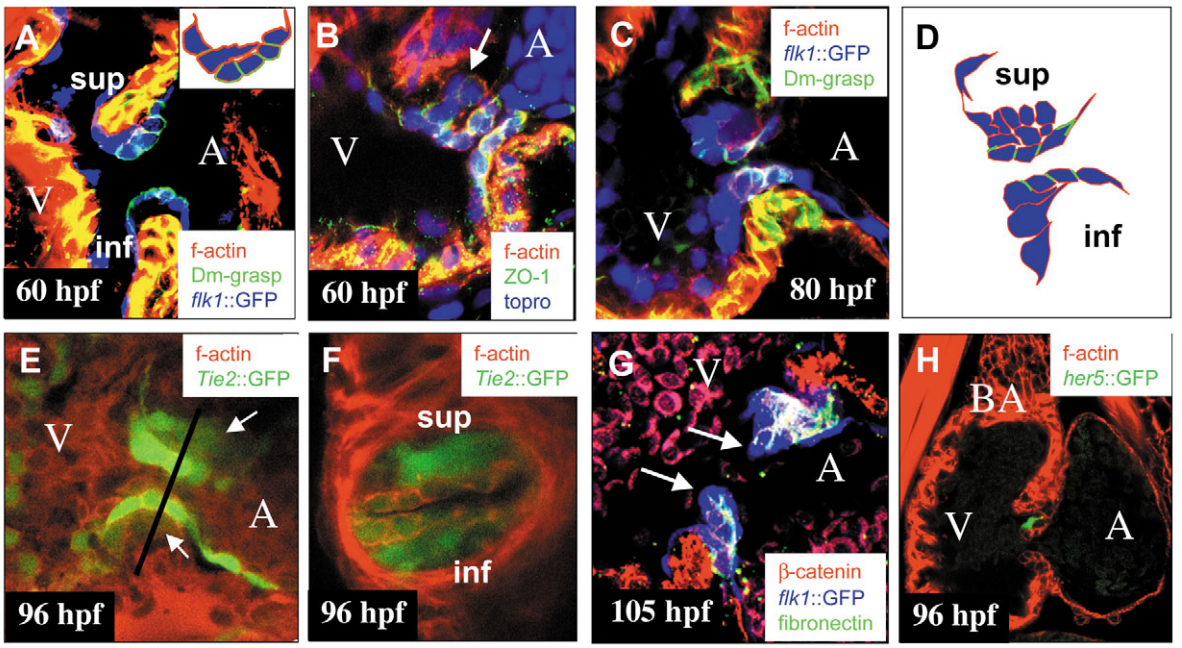

Fig. 2. Wild-type endocardial cushion morphogenesis. Confocal images of the AV canal at 60 (A,B), 80 (C), 96 (E,F) and 105 hpf (G), and of the heart at 96 hpf (H). (A,C,G) *Tg(flk1:EGFP)*^{s843} (pseudo-colored blue) embryo immunostained for Dm-grasp (pseudo-colored green) and stained with rhodamine phalloidin (red) (A,C) or immunostained for fibronectin (pseudo-colored green) and β catenin (red) (G). (E,F) *Tg(Tie2:EGFP)*^{s849} (green) embryo stained with rhodamine phalloidin (red). (B) Embryo immunostained for ZO-1 (green) and stained with topro (blue) and rhodamine phalloidin (red). (H) *Tg(0.7her5:EGFP)*^{ne2067} (green) embryo stained with rhodamine phalloidin (red). (A) AV endocardial cell at the ventricular border has extended into the ECM and is reaching the base of cells close to the atrial border. Inset shows schematic drawing of AV endocardial cells of the superior AV EC. (B) Cells, such as the one indicated by the arrow, located in the ECM between the endocardium and myocardium have downregulated and delocalized ZO-1, indicating an epithelial to mesenchymal transition. (C) At 80 hpf, the superior AV EC consisting of mesenchymal cells has formed. In the inferior ECFR at this time, AV endocardial cells at the ventricular border start extending cellular protrusions into the ECM. (D) Schematic representation of AV canal endocardial cells as shown in C. (E,F) By 96 hpf, both superior and inferior AV ECs (arrows in E) have formed. Line in E indicates the plane of the transverse section shown in F. (G) By 105 hpf, ECs have elongated and start projecting into the ventricular lumen. Cushion extensions (arrows) consist of two layers of cells separated by a layer of fibronectin-containing ECM. (H) Expression of *Tg(0.7her5:EGFP)*^{ne2067} in a subset of cells in elongating ECs. A, atrium; BA, bulbus arteriosus; V, ventricle; inf, inferior AV EC; sup: superior AV EC.

superior (i.e. anteriormost) EC-forming region (ECFR), and the region adjacent to the outer curvature of the ventricle as the inferior ECFR. ECs formed in the corresponding regions are referred to as superior and inferior ECs.

In a transverse section through the AV canal at 55 hpf, a single sheet of cuboidal endocardial cells can be seen lining the superior and another sheet lining the inferior ECFR of the AV canal (Fig. 1F). Laterally, these two sheets are interconnected by squamous cells, which we refer to as hinge cells. There are approximately 40 cuboidal endocardial cells (one sheet of 20 cells in each ECFR) in the AV canal at this stage.

Endocardial cushion formation and valve morphogenesis

In order to understand how ECs form, we analyzed subsequent stages of heart development. By 60 hpf in the superior region of the AV canal, endocardial cells located at the border with the ventricle have formed cellular extensions that project into the ECM between the endocardium and myocardium, reaching towards the base of cells located at the border between the AV canal and atrium (Fig. 2A, n=11). These data indicate that endocardial cells on the two different boundaries of the AV canal have distinct developmental properties and behavior.

We tested whether AV endocardial cells undergo EMT after sending cellular protrusions into the ECM, by immunostaining 60 hpf embryos for ZO1. Fig. 2B shows that endocardial cells in the ECM (arrow) have downregulated and delocalized ZO1, indicative of EMT. In the superior region of the AV canal, an EC forms on the basal side of a single layer of cuboidal Dm-grasp positive endocardial cells (Fig. 2C,D, n=6). The endocardial cells at the ventricular border of the inferior region of the AV canal begin to form cellular extensions into the ECM at 80 hpf in a pattern similar to that observed in the superior cushion, indicating a delayed initiation of the formation of the inferior EC relative to the superior one (Fig. 2D). By 96 hpf, both cushions have formed (Fig. 2E, arrows). In transverse sections, the mesenchymal cushions are located between the AV myocardium and a layer of cuboidal endocardium (Fig. 2F). AV ECs are transient structures; by 105 hpf, both cushions have started morphogenetic rearrangements that ultimately lead to the formation of the valve leaflets (Fig. 2G,H). Both AV ECs extend into the ventricular lumen (Fig. 2G, arrows). These extensions consist of an outgrowth formed by two layers of cells separated by a layer of fibronectin-containing ECM (Fig. 2G). At 96 hpf, we also observe *Tg(0.7her5:EGFP)*^{ne2067} expression in a subset of cells in the extending ECs (Fig. 2H). *Tg(0.7her5:EGFP)*^{ne2067} expression is observed in a subpopulation of AV canal endocardial cells from 48 until 120 hpf (data not shown), although the biological significance of this expression is unclear at this time.

At 7 days post-fertilization (dpf), both ECs have transformed into leaflets with two distinct cell layers (Fig. 3B, arrowheads). These leaflets are connected laterally to the trabeculae of the ventricular myocardium (Fig. 3A, arrowheads, Fig. 3C). In addition, the superior AV valve leaflet is connected to the AV myocardium by a row of cuboidal Dm-grasp-positive cells (Fig. 3B, arrow). By their position, these cells could be analogous to the AV septum in mammalian hearts. The valve leaflets retain their two cell-layer thickness at least until 28 dpf

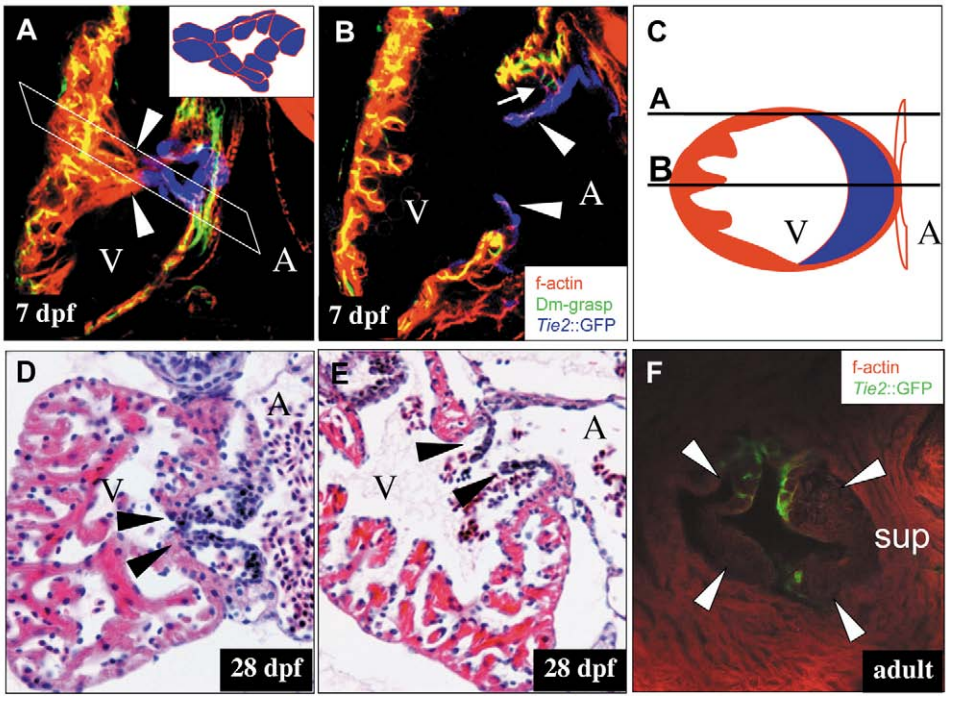

Fig. 3. Wild-type morphogenesis of AV valve leaflets. (A,B) Confocal images of the AV canal at 7 dpf. (C) Schematic drawing of a transverse section through the ventricle at the level of a valve leaflet. (D,E) Hematoxylin and Eosin-stained sections through the AV canal at 28 dpf. (F) Adult valve leaflets. (A,B) Sections of a *Tg(Tie2:EGFP)*^{s849} (pseudo-colored blue) heart immunostained for Dm-grasp (pseudo-colored green) and stained with rhodamine phalloidin (red). (A) Optical section through the lateral wall of the ventricle as indicated in C shows that each of the two leaflets is connected to distal ventricular myocardial trabeculae (arrowheads). White parallelogram indicates the plane schematically depicted in C. (B) Optical section through the ventricle as indicated in C. Valve leaflets consist of two layers of *Tg(Tie2:EGFP)*^{s849} positive cells (arrowheads). The myocardial wall distal to the AV canal is trabeculated in contrast to the juxtavalvular ventricular wall. The superior valve leaflet (arrow) is connected to the AV myocardium by a row of weakly *Tg(Tie2:EGFP)*^{s849}-positive (i.e. endocardially derived) cuboidal cells that express Dm-grasp (arrow). (C) Lines labeled A and B represent the approximate latitude of the optical sections shown in A and B, respectively. (D) Oblique section through the AV canal shows that the valve leaflets (arrowheads) are connected laterally to the ventricular trabeculae. (E) Sagittal section through the heart shows that the valve leaflets consist of two layers of cells (arrowheads). (F) The adult zebrafish AV valve consists of four leaflets (arrowheads). A, atrium; V, ventricle; sup, superior AV valve leaflets.

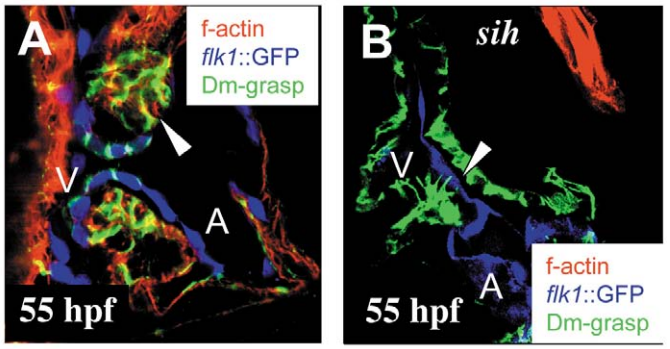

Fig. 4. Regulation of AV endocardial development. Confocal images of the AV canal of wild-type (A) and mutant (B) hearts at 55 hpf. (A,B) *Tg(flk1:EGFP)*^{s843} (pseudo-colored blue) embryos immunostained for Dm-grasp (pseudo-colored green) and stained with rhodamine phalloidin (red). In contrast to wild type (A), in *sih* mutant embryos (B), AV canal endocardial cells (arrowhead) fail to express Dm-grasp and to adopt a cuboidal shape. Interestingly, the *sih* mutant myocardium is devoid of filamentous actin staining. A, atrium; V, ventricle.

(Fig. 3D,E). By the adult stage, the AV valve has four leaflets (Fig. 3F).

Regulation of AV canal differentiation

We recently reported that in *sih* mutant embryos, the AV canal endocardium fails to upregulate *Tg(Tie2:EGFP)*^{s849} expression (Bartman et al., 2004). In order to analyze in detail the cellular basis for this phenotype, we examined Dm-grasp expression in *Tg(flk1:EGFP)*^{s843} *sih* mutant embryos. We found that in these embryos AV canal endocardial cells remain squamous and fail to express Dm-grasp (Fig. 4B). These data indicate that the contractility of the heart is required for the AV canal endocardium to adopt a cuboidal organization and express Dm-grasp.

Notch signaling restricts the differentiation of cuboidal endocardium to the AV canal

In zebrafish embryonic hearts, *notch1b* expression is distributed throughout the ventricular endocardium at 24 hpf and then becomes restricted to the AV canal endocardium around 48 hpf (Walsh and Stainier, 2001; Westin and Lardelli, 1997). In *jek*

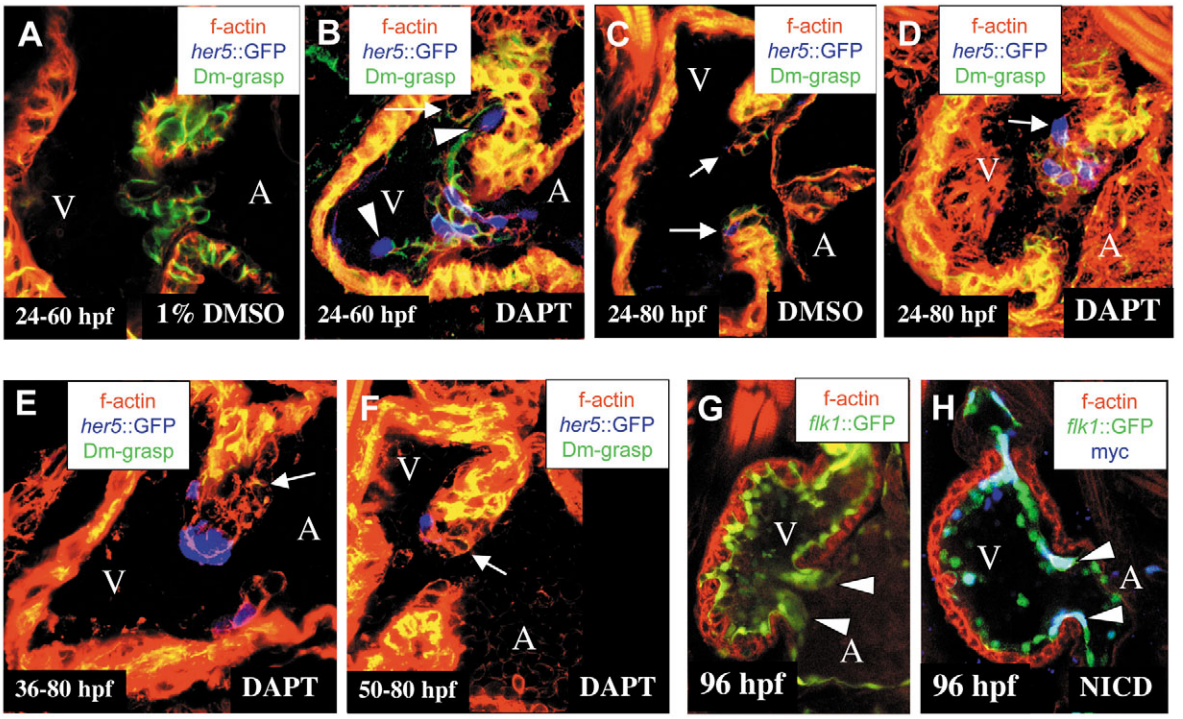

Fig. 5. Notch signaling restricts the differentiation of cuboidal endocardium to the AV canal. Confocal images of hearts from DMSO-treated (A,C) and DAPT-treated embryos (B,D-F) at 60 (A,B) and 80 hpf (C-F), and from wild-type (G) and NotchICD-overexpressing (H) embryos at 96 hpf (G,H). (A-F) *Tg(0.7her5:EGFP)*^{ne2067} embryos (pseudo-colored blue) immunostained for Dm-grasp (pseudo-colored green) and stained with rhodamine phalloidin (red). (G,H) *Tg(flk1:Gal4-UAS:EGFP)*^{s848} (green) (G) and transheterozygous *Tg(flk1:Gal4-UAS:EGFP)*^{s848} (green); *Tg(UAS:myc-Notch1a-intra)*^{kca3} (H) embryos immunostained for MYC (blue) and stained with rhodamine phalloidin (red). (Most endocardial cells stained positive for MYC expression although the AV canal endocardial cells appear to express higher levels.) (A) In embryos treated with 1% DMSO, cuboidal, Dm-grasp positive endocardial cells were restricted to the AV canal. (B) In embryos treated with 100 μM DAPT between 24-60 hpf, the ventricular endocardium showed ectopic cuboidal, Dm-grasp-positive cells (arrow) and ectopic *Tg(0.7her5:EGFP)*^{ne2067} expression (arrowheads). (C) In embryos treated with 1% DMSO from 24-80 hpf, EC development was unaffected, and *Tg(0.7her5:EGFP)*^{ne2067} expression was restricted to single cells located at the boundary between the ventricle and AV canal (arrows). Embryos treated with 100 μM DAPT from 24-80 hpf (D) formed a hypercellular EC in the superior region of the AV canal with numerous *Tg(0.7her5:EGFP)*^{ne2067}-positive cells. Embryos treated from 36-80 hpf (E) and from 50-80 hpf (F) formed a disorganized cushion similar to the control in size and cell numbers (compare with C) although with reduced Dm-grasp expression in the cuboidal endocardial cells (arrows). (G) *Tg(flk1:Gal4-UAS:EGFP)*^{s848} embryos have completed the formation of the superior and inferior AV canal ECs by 96 hpf (arrowheads). (H) NotchICD-expressing AV canal endocardial cells (arrowheads) remain squamous, resulting in a lack of AV canal ECs at 96 hpf.

Development

(*ugdh*) mutant embryos, which fail to form ECs, this restriction of *notch1b* expression fails to occur (Walsh and Stainier, 2001). In a recent study, Notch1 signaling has been shown to be required for the progression of differentiation of the endocardium in mouse (Timmerman et al., 2004). In order to test whether Notch signaling is required for the regulation of AV canal endocardial cell differentiation, we manipulated Notch signaling in the *Tg(0.7her5:EGFP)*^{ne2067} background. We incubated *Tg(0.7her5:EGFP)*^{ne2067} embryos with different concentrations of the γ-secretase inhibitor DAPT. γ-Secretase is required for the activation of the Notch signaling pathway (reviewed by Mumm and Kopan, 2000) and DAPT-treated zebrafish embryos have somitogenesis and neurogenesis phenotypes identical to those caused by a loss of Notch signaling (Geling et al., 2002). We found that zebrafish embryos treated with 10 and 100 μM DAPT from 24-60 hpf exhibited ectopic expression of Dm-grasp in endocardial cells throughout the ventricular chamber at 60 hpf (10 μM DAPT n=5; 100 μM DAPT n=8). These cells had characteristics of AV canal endocardial cells such as a cuboidal appearance and upregulated actin staining (Fig. 5B, arrow). In addition, some of the ectopic Dm-grasp-positive cells also expressed *Tg(0.7her5:EGFP)*^{ne2067} (Fig. 5B, arrowheads). These results indicate that Notch signaling is required in the ventricular endocardial cells to maintain their squamous morphology and inhibit an AV canal fate. When embryos were treated with 100 μM DAPT from 24 to 80 hpf, embryonic hearts formed hypercellular ECs in the superior region of the AV canal (Fig. 5D, arrow, n=8), suggesting that inhibiting Notch signaling does not block EC formation. These hypercellular cushions could result from the aggregation of supernumerary cuboidal endocardial cells or a hyperactivation of EMT. In order to test whether DAPT treatments affect EMT, as has been suggested previously (Timmerman et al., 2004), we treated embryos between 36-80 hpf (n=6) and 50-80 hpf (n=12). We found that in both cases, ECs were comparable in size to the DMSO controls (n=11), although they appeared disorganized and Dm-grasp expression was downregulated in cuboidal endocardial cells (Fig. 5E,F). These data indicate that Notch signaling regulates cell differentiation and patterning during AV canal EC formation.

In order to test whether constitutive Notch signaling is sufficient to inhibit AV canal endocardial cell differentiation, the intracellular domain of Notch was expressed in all endothelial cells of the zebrafish embryo using the GAL4/UAS binary expression system. *Tg(flk1:Gal4-UAS:EGFP)*^{s848} fish were crossed with the *Tg(UAS:myc-Notch1a-intra)*^{kca3} line (Scheer, 1999). Immunostaining for the myc-tag was used to visualize embryos positive for myc-Notch-intra (Fig. 5H, blue; there is overlap with EGFP, which is also under the control of *flk1*:GAL4). These experiments showed an absence of cuboidal cells and ECs in the AV canal at 96 hpf (Fig. 5H; n=12). By contrast, wild-type embryos have fully developed ECs at 96 hpf (Fig. 5G, arrowheads). These data show that constitutive activation of Notch signaling in endocardial cells is able to suppress their transition from squamous to cuboidal, an essential step for EC development.

Calcineurin signaling is required for AV endocardium EMT and subsequent valve morphogenesis

Chang et al. (Chang et al., 2004) recently reported that myocardial NFATc through suppression of VEGF signaling allows EMT to occur and that subsequent NFATc signaling is required for proper valve morphogenesis. Using the tools reported in this paper, we wanted to further analyze the cellular basis for these requirements. We observed that raising zebrafish embryos from the one cell stage in medium with 10 μg/ml CsA, which blocks NFATc signaling, resulted in a very specific heart defect with no other obvious morphological phenotypes (Fig. 6A; n>100). Embryos developed outflow tract stenosis and blood regurgitation between the atrium and ventricle by 60 hpf (Fig. 6A; see Movie 1 in the supplementary material). The myocardium appeared thinner at 96 hpf, as

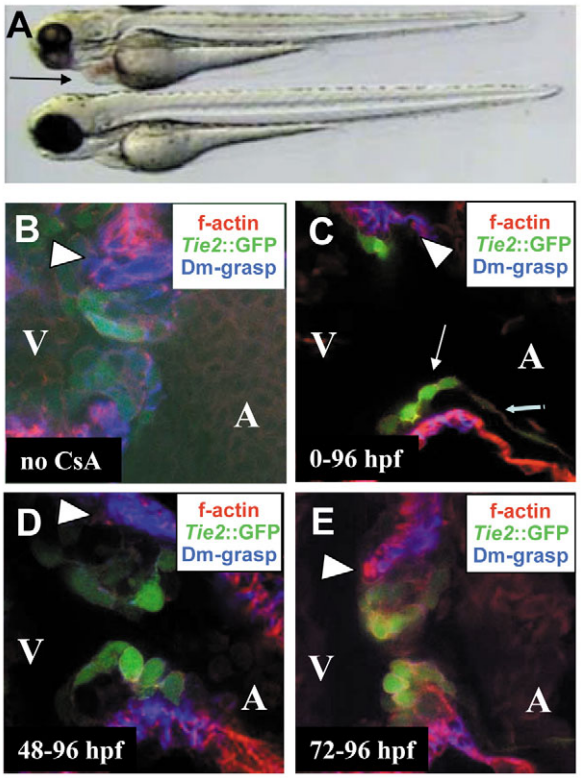

Fig. 6. Calcineurin signaling is required for EMT and EC morphogenesis. (A) Bright-field image of an untreated embryo (bottom) and an embryo raised in 10 μg/ml CsA (top). (B-E) Confocal images of the AV canal of *Tg(Tie2:EGFP)*^{s849} (green) embryos at 96 hpf immunostained for Dm-grasp (blue) and stained with rhodamine phalloidine (red); (B) untreated embryo; (C-E) embryos treated with CsA from the one cell stage (C), 48 hpf (D) and 72 hpf (E). (A) Embryos treated with CsA from the one cell stage appeared morphologically wild type at 72 hpf, except for pericardial edema (arrow in A) owing to outflow tract stenosis (see Movie 1 in the supplementary material). (C) In embryos treated with CsA from the one-cell stage, the myocardium appeared thinner throughout the heart (compare with B, D, E and Fig. 2). AV endocardial cells upregulated *Tg(Tie2:EGFP)*^{s849} and initiated a cell shape change (thin arrow indicates AV endocardial cell, thick arrow indicates squamous atrial endocardial cell), but failed to express Dm-Grasp; no EMT occurred and ECs failed to form. (D) In embryos treated with CsA from 48 hpf, ECs appeared disorganized. (E) No effect on EMT or cushion morphogenesis was observed at 96 hpf when embryos were treated with CsA from 72 hpf onwards (compare E with B). Arrowheads indicate the superior region of the AV canal in B-E.

Table 1. Summary of the mutants identified in our forward genetic screen

Phenotypic groups	Alleles	Loci (CG)	Heart defects	Previously identified loci
Cellular organization defects	4	4	Cell morphology defects	*oko meduzy* (*ome*)
Left-right asymmetry, random heart jogging	2	2	Random heart and endodermal organ positioning at 36 hpf	
Large heart	2	2	AV mis-specification	*santa* (*san*), *valentine* (*vtn*)
Blood regurgitation at the AV canal	12	10	Outflow tract stenosis, lack of cuboidal AV endocardium	
Ventricular defects cause sinoatrial regurgitation	17	13	Noncontracting ventricle, collapsed ventricle, ventricle fails at 80 hpf	
Sinoatrial regurgitation without obvious ventricular defects	6	6	Excessive ECM between endocardial/myocardial cells, lack of ECs	
Heart fins and jaw defects	5	5	Lack of ECs	*hands off* (*han*), logelei (log)
Day 4 heart defects	7	6	AV cushion and atrial endocardium defects	
Total (in eight groups)	55	48		5

The mutants exhibit atrioventricular (AV) or sinoatrial blood regurgitation at 48 or 96 hpf. Groups are ordered according to the time of appearance of the regurgitation phenotype, from earlier to later. Allele numbers of each one and mapping positions for a subset of the mutants is in Table S1 in the supplementary material. CG, complementation group.

previously described (Molkentin et al., 1998) and had little to no trabeculae (compare Fig. 6C with 6B). However, despite these myocardial defects, contractility appeared unaffected up to 96 hpf (see Movie 1 in the supplementary material). Interestingly, although AV endocardial cells initiated cell shape changes and upregulated *Tg(Tie2:EGFP)*^{s849} (Fig. 6C, arrows; n>10), they failed to undergo EMT and form ECs (Fig. 6C, arrows). Applying CsA at 48 hpf did not interfere with the initiation of EMT but resulted in disorganized ECs (Fig. 6D; n>10), supporting the report of an additional, later role of NFATc signaling in mouse valve morphogenesis (Chang et al., 2004).

Forward genetic screen for AV canal defective mutants

Although in previous large-scale mutagenesis screens over 130 mutations affecting heart development have been identified, only single alleles of AV canal defective mutants like *jekyll* or *cardiofunk* have been found (Bartman et al., 2004; Walsh and Stainier, 2001), indicating a lack of saturation for such phenotypes. In order to identify new regulators of zebrafish heart morphogenesis, we carried out a large-scale ENU mutagenesis screen. Intercrosses of F2 families were screened by visual inspection of live embryos between 50 and 60 hpf, and on day 5-6 postfertilization for retrograde blood flow through the heart and defective heart morphology. F2 carriers of putative mutations were outcrossed with *Tg(Tie2:EGFP)*^{s849} or *Tg(flk1:EGFP)*^{s843} fish to facilitate the cellular analysis of endocardial cells. Recovered mutations were organized into phenotypic groups and tested by complementation analysis. The results are summarized in Table 1. We screened a total of 9076 clutches, from 2392 families (representing 2723 mutagenized genomes) and identified 55 mutations. Five mutations were allelic to previously identified loci. The other 50 potentially novel mutations fell into 43 complementation groups. On average, we found 1.1 alleles per locus. Although this number does not allow the estimation of the degree of saturation of our screen, it indicates that additional zebrafish genes that when mutated give a cardiac morphogenesis phenotype remain to be identified. Blood regurgitation was used in the forward genetic screen as an indicator for a defect in the form and function of the developing valve. Further analysis of the cardiac phenotype by rhodamine phalloidin staining of *Tg(Tie2:EGFP)*^{s849} or *Tg(flk1:EGFP)*^{s843} embryos allowed us to order these mutations according to the affected process. Analyses at the cellular level revealed that mutations in this group disrupt different stages and aspects of EC development, and show that the developing ECs function to ensure unidirectional blood flow days before the valve leaflets have formed. Representative examples of phenotypes observed in the screen are described below.

AV canal differentiation is affected in the *s204* mutant, as AV canal endocardial cells remained squamous although expressing wild-type levels of *Tg(Tie2:EGFP)*^{s849} (Fig. 7B). This observation indicates that the *s204* mutation specifically causes a defect in the squamous to cuboidal transformation of AV canal endocardial cells.

In contrast to the *s204* phenotype, the *s22* mutation causes the ventricular lumen to be filled with cuboidal *Tg(Tie2:EGFP)*^{s849}-expressing cells (Fig. 7C). This observation suggests that endocardial cells in the ventricle undergo an ectopic differentiation reminiscent of AV canal endocardial cells. The cellular structure of the atrium in *s22* mutant embryos appears normal with squamous endocardial and myocardial cells. We observed a somewhat similar phenotype in the *apc* mutant (Hurlstone et al., 2003) where the atrium appears normal, while the ventricular endocardial cells appear mesenchymal and fill the ventricular lumen (Fig. 7D).

In *s624* mutant embryos at 72 hpf, AV endocardial cells form extensions into the ECM in a disorganized fashion and the ECs are absent (Fig. 7F). The *s624* phenotype suggests that a tight spatial regulation of the behavior of these cells is important for AV cushion morphogenesis.

The *s266* mutation results in a single layer of cuboidal endocardial cells in the AV canal as late as 96 hpf with no

Development

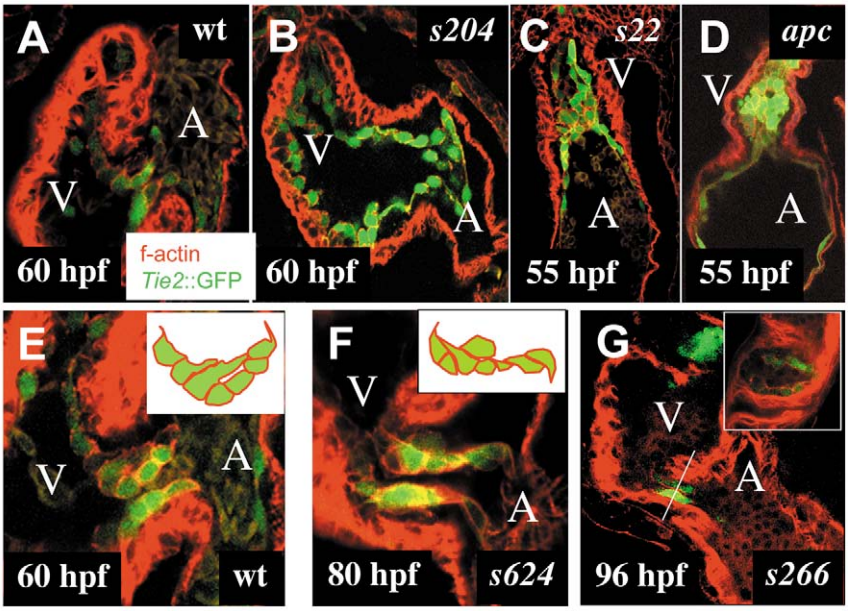

Fig. 7. AV canal defective mutants identified in a large-scale mutagenesis screen. Wild-type (A,E) and mutant (B-D,F,G) hearts between 55 and 96 hpf. Confocal images of embryonic hearts at 60 (A,B) and 55 hpf (C,D). Confocal images of the AV canal at 60 (E), 80 (F) and 96 hpf (G). In contrast to wild-type hearts at 60 hpf (A), in *s204* mutant hearts (B), the AV canal endocardial cells fail to adopt a cuboidal shape. (C) In *s22* mutant hearts, the ventricular lumen contains cuboidal endocardial cells. (D) In the *apc* mutant heart, the ventricular lumen is filled with *Tg(Tie2:EGFP)*^{s849}-positive cells with a mesenchymal morphology. (E) In wild-type embryos, only AV canal endocardial cells located next to the ventricular border form cellular extensions into the AV canal ECM and extensions are directed towards the atrial border of the AV canal. (F) In *s624* mutant embryos at 80 hpf, no ECs have formed, and the AV canal endocardial cells extend cellular projections in different directions. (G) In *s266* mutant embryos, no ECs have formed by 96 hpf; the AV canal is lined by a single layer of cuboidal cells. Inset shows a transverse section of the *s266* mutant AV canal (compare with Fig. 2F and see Movie 2 in the supplementary material). A, atrium; V, ventricle.

cellular extensions observed (Fig. 7G). These data indicate that the *s266* gene is required for the physical process of EMT during EC formation.

Discussion

As has been described in amniotes, AV valve development in zebrafish progresses through three stages: (1) differentiation of the cells lining the AV canal; (2) formation of ECs through the EMT of a subset of AV endocardial cells; and (3) subsequent morphogenesis of ECs into valve leaflets. During all these stages, the developing heart is pumping blood, while the AV region functions to prevent retrograde blood flow even during its own morphogenetic transformation.

AV canal differentiation

In mouse and chick embryos, the differentiation of the AV canal comprises not only a thickening of the ECM in the AV canal but also the acquisition of specific developmental properties by both endocardial and myocardial cells in this region (reviewed by Eisenberg and Markwald, 1995). Similarly, we find that in zebrafish embryos, endocardial and myocardial cells differentiate morphologically before the onset of EMT. The AV endocardium undergoes a transition from squamous to cuboidal cell shape and starts expressing Dm-grasp, a cell-adhesion molecule that becomes localized laterally. Cuboidal AV endocardial cells show a characteristic pattern of actin and β-catenin staining indicative of adherens junctions. This process starts around 36 hpf and is completed by 55 hpf, when the superior and inferior regions of the AV canal are each lined by a sheet of cuboidal endocardial cells interconnected by squamous cells. As the AV canal must function to ensure unidirectional blood flow prior to the formation of the cushions or valves proper, we suggest that this spatial organization of squamous and cuboidal cells is required to prevent blood regurgitation. Others have shown that at 4.5 dpf the diameter of the AV canal changes 2.8-fold between systole and diastole (Hove et al., 2003). It is likely that the specific arrangement of cuboidal and squamous cells allows for this change in diameter and that the two opposing sheets of cuboidal cells ensure closure of the AV canal during ventricular systole.

In chick, rat and mouse embryos, ‘rounded’ AV endocardial cells have been described to extend cellular protrusions into the ECM, a hallmark for the onset of EMT (Markwald et al., 1977; Timmerman et al., 2004). A recent report has identified an early pro-valve enhancer in the first intron of *NFATc1*. This enhancer is active specifically in endocardial cells at the AV boundary and the outflow tract at stages before EMT, and not in transformed endocardial cells invading the ECM (Zhou et al., 2005). These data suggest that this enhancer marks the mammalian equivalent of the earliest Dm-grasp-positive AV endocardial cells reported here. Other cuboidal endothelial cells have been described in the high endothelial venules (HEV) present in the paracortex of lymph nodes, tonsils and interfollicular areas of Peyer’s patches. HEVs are lined by a high-walled endothelium that functions in the homing of lymphocytes (Miyasaka and Tanaka, 2004). The function of zebrafish cuboidal endocardium is obviously different from that of HEVs. The transition of a squamous to cuboidal endocardium in the AV canal of zebrafish is another milieu in which basic cell biological questions regarding the regulation of changes in cell shape, organization and cell-cell adhesion can be addressed.

Differentiation of AV canal endocardial cells depends on cardiac contractility

We analyzed the role of mechanical function of the heart in AV canal endocardial cell differentiation. We find that in *sih* mutants, which lack heart contraction, AV canal endocardial cells fail to express Dm-grasp and to change shape. It remains to be determined whether the required mechanical stimulus comes from the wall forces of heart muscle contraction or from

Development

hemodynamic shear stress (reviewed by Bartman and Hove, 2005). In cell culture, bovine aortic endothelial cells respond to shear stress by changing cytoskeletal organization, cell-adhesion complexes, cell morphology and gene expression (reviewed by McCue et al., 2004). Intra-cardiac shear stress can be calculated by indirect methods in live embryonic zebrafish hearts, and in the 37 hpf embryonic heart wall shear forces of 2.5 dyn/cm^2 have been estimated (Hove et al., 2003). Hemodynamic shear stress is therefore a good candidate to cause changes in endocardial cell shape, adhesion and gene expression. Likewise, passive cyclical mechanical stretch of skeletal myocytes in culture (i.e. in the absence of flow) appears to be sufficient to transdifferentiate these cells into cardiomyocytes (Iijima et al., 2003). It has not been tested whether similar mechanical forces in the absence of flow can also affect the differentiation of endothelial cells. Future experiments should address the source and role of shear stress in the differentiation of AV canal cells, and aim to identify the molecular triggers for this process.

Notch and calcineurin signaling are involved in the spatiotemporal control of AV canal specification and differentiation

The characteristic changes in cell shape and organization together with the specific expression of Dm-grasp are reliable markers for the specification and differentiation of the AV canal endocardial cells. Here, we made use of these cellular and molecular changes to show that Notch signaling is required to restrict this program of differentiation to the endocardial cells of the AV canal. When Notch signaling was inhibited by DAPT treatment, cells with AV canal endocardial morphology and protein expression were found within the ventricle. Conversely, constitutive activation of Notch signaling inhibited the transition of AV endocardial cells from squamous to cuboidal, as well as the subsequent formation of ECs by EMT. These results indicate that Notch signaling inhibits the differentiation of the ventricular endocardium into cells with AV canal-like, cuboidal, Dm-grasp-expressing properties.

A different experimental protocol, the early and widespread expression of NotchICD following mRNA injection at the one-cell stage, led to hypertrophic ECs, suggesting that Notch activation induces excessive EMT (Timmerman et al., 2004). However, this approach resulted in a high mortality rate (80% by 48 hpf). In our experiments, the use of the GAL4/UAS system to express NotchICD only in endocardial/endothelial cells from ~24 hpf onwards avoids the indirect effects associated with mRNA injections. Indeed, *Tg(flk1:Gal4-UAS:EGFP)^{s848}; Tg(UAS:myc-Notch1a-intra)^{kca3}* embryos exhibited pericardial edema starting at 3 dpf but appeared unaffected otherwise and survived up to 7 dpf, without developing any ECs. Our observations with DAPT treatments were also different from those reported by Timmerman et al. (Timmerman et al., 2004). Whereas they reported that treating embryos with 50-100 μM DAPT from 36 hpf to 5 dpf resulted in the formation of atrophied cushions, in our hands, such treatment led to 100% lethality by 96 hpf in two independent experiments. Therefore, we reduced the exposure time and found that DAPT treatments from 36 to 80 hpf and from 50 to 80 hpf resulted in the formation of normal size superior ECs. However, these ECs appeared disorganized and Dm-grasp was downregulated in the cuboidal endocardial cells, suggesting that Notch signaling is required to maintain the correct pattern of cell fates in the forming EC. It is possible that this function of Notch signaling is required to maintain an efficient development and/or growth of ECs from 60 to 96 hpf, which would explain the atrophied appearance of the ECs by Timmerman et al. (Timmerman et al., 2004). These data indicate, in a model consistent with the pattern of *notch1b* expression in the endocardium, that Notch signaling plays multiple roles in EC formation, starting with the repression of the AV canal endocardial phenotype in the ventricle.

Work in mouse has shown that while the later steps of EMT require NFATc1 function in endocardial cells, at earlier stages myocardial Vegf expression is repressed by NFATc2/3/4 signaling and this repression is required for EMT initiation (Chang et al., 2004). Inhibiting calcineurin function from an early stage in zebrafish embryos blocked the differentiation of the AV canal endocardium (as demonstrated by the absence of Dm-grasp expression in the AV canal endocardial cells and their failure to undergo EMT). However, some aspects of AV canal specification, as illustrated by the *Tg(Tie2:EGFP)^{s849}* upregulation, were not affected. These results suggest that calcineurin signaling is also required for the differentiation of the AV endocardium.

Systematic analysis of the identified mutants will help elucidate mechanisms of cushion and valve morphogenesis

Our data show that in zebrafish, as in amniotes, ECs are formed by the migration into the ECM of a subset of AV canal endocardial cells followed by their EMT. We found that only AV endocardial cells located at the ventricular boundary migrate in the direction of the atrial boundary. This finding suggests that cells along the AV canal have different developmental properties, whereby only cells at the ventricular boundary are able to respond to a localized guidance cue coming from the direction of the atrial boundary. Detailed analysis of EC morphogenesis mutants such as *s266* and *s624* will be instrumental in understanding the underlying molecular and cellular mechanisms of these processes.

AV ECs are transient structures in zebrafish embryos. Their formation begins around 60 hpf and their transformation into valve leaflets around 96 hpf. In comparison to the four-chambered hearts of mouse and chick, where ECs are involved in both the development of valves and interventricular and interatrial septae, in the zebrafish heart valve morphogenesis is a simpler process giving rise initially to two leaflets and the AV septum. At a later stage, the two valve leaflets in the AV canal are remodeled to give rise to four leaflets.

The power of the zebrafish system revolves around its amenability to forward and reverse genetics, as well as several methods for studying organogenesis at the cellular level, allowing a high degree of integration of genetic and cellular studies. In our screen, we identified mutations affecting distinct stages of AV cushion development. The systematic analysis of this mutant collection will be instrumental in furthering our understanding of the molecular regulation of AV canal differentiation and subsequent valve development. Furthermore, zebrafish embryos are also ideal for the pharmacological analysis of specific signaling pathways in various developmental processes. The combination of genetic and pharmacological studies, along with detailed analyses of

the cell biology of cushion/valve development, should provide novel insights into the developmental biology of cardiac organogenesis and provide relevant information to the clinicians who care for individuals with valvular and septal malformations.

We thank all the members of the Baier and Stainier laboratory screen teams for their support during the screens; Steve Waldron, Natasha Zvenigorodsky and Ana Ayala for expert help with the fish; and Paul Scherz and Le Trinh for critical comments on the manuscript. D.B. and H.V. were supported by long-term fellowships from the HFSPO; E.A.O., S.W.J. and L.A.D. by Postdoctoral fellowships from the AHA; B.J. by a Otto Hahn Medal fellowship from the Max-Planck Gesellschaft and a postdoctoral fellowship from the AHA; T.B. by a Postdoctoral fellowship for Physicians from HHMI; and I.A.C. by a Postdoctoral fellowship from the Canadian MRC. H.B. and J.N.C. are supported by grants from the NIH, and L.B.C. by the Volkswagenstiftung. This work was supported in part by grants from the NIH (NHLBI), the AHA and the Packard Foundation to D.Y.R.S.

Supplementary material

Supplementary material for this article is available at
http://dev.biologists.org/cgi/content/full/132/18/4193/DC1

References

Armstrong, E. J. and Bischoff, J. (2004). Heart valve development: endothelial cell signaling and differentiation. *Circ. Res.* **95**, 459-470.

Bartman, T. and Hove, J. (2005). Mechanics and function in heart morphogenesis. *Dev. Dyn.* **233**, 373-381.

Bartman, T., Walsh, E. C., Wen, K. K., McKane, M., Ren, J., Alexander, J., Rubenstein, P. A. and Stainier, D. Y. (2004). Early myocardial function affects endocardial cushion development in zebrafish. *PLoS Biol.* **2**, 673-681.

Basson, C. T., Bachinsky, D. R., Lin, R. C., Levi, T., Elkins, J. A., Soults, J., Grayzel, D., Kroumpouzou, E., Traill, T. A., Leblanc-Straceski, J., Renault, B., Kucherlapati, R., Seidman, J. G., Seidman, C. E. (1997). Mutations in human TBX5 cause limb and cardiac malformation in Holt-Oram syndrome. *Nat. Genet.* **15**, 30-35.

Bernanke, D. H. and Markwald, R. R. (1982). Migratory behavior of cardiac cushion tissue cells in a collagen-lattice culture system. *Dev. Biol.* **91**, 235-245.

Chang, C. P., Neilson, J. R., Bayle, J. H., Gestwicki, J. E., Kuo, A., Stankunas, K., Graef, I. A. and Crabtree, G. R. (2004). A field of myocardial-endocardial NFAT signaling underlies heart valve morphogenesis. *Cell* **118**, 649-663.

de la Pompa, J. L., Timmerman, L. A., Takimoto, H., Yoshida, H., Elia, A. J., Samper, E., Potter, J., Wakeham, A., Marengere, L., Langille, B. L., Crabtree, G. R., Mak, T. W. (1998). Role of the NF-ATc transcription factor in morphogenesis of cardiac valves and septum. *Nature* **392**, 182-186.

Eisenberg, L. M. and Markwald, R. R. (1995). Molecular regulation of atrioventricular valvuloseptal morphogenesis. *Circ. Res.* **77**, 1-6.

Fashena, D. and Westerfield, M. (1999). Secondary motoneuron axons localize DM-GRASP on their fasciculated segments. *J. Comp. Neurol.* **406**, 415-424.

Garg, V., Kathiriya, I. S., Barnes, R., Schluterman, M. K., King, I. N., Butler, C. A., Rothrock, C. R., Eapen, R. S., Hirayama-Yamada, K., Joo, K., Matsuoka, R., Cohen, J. C. and Srivastava, D. (2003). GATA4 mutations cause human congenital heart defects and reveal an interaction with TBX5. *Nature* **424**, 443-447.

Geling, A., Steiner, H., Willem, M., Bally-Cuif, L. and Haass, C. (2002). A gamma-secretase inhibitor blocks Notch signaling in vivo and causes a severe neurogenic phenotype in zebrafish. *EMBO Rep.* **3**, 688-694.

Gruber, P. J. and Epstein, J. A. (2004). Development gone awry: congenital heart disease. *Circ. Res.* **94**, 273-283.

Hacker, U., Lin, X. and Perrimon, N. (1997). The Drosophila sugarless gene modulates Wingless signaling and encodes an enzyme involved in polysaccharide biosynthesis. *Development* **124**, 3565-3573.

Hoffman, J. I. and Kaplan, S. (2002). The incidence of congenital heart disease. *J. Am. Coll. Cardiol.* **39**, 1890-1900.

Hove, J. R., Koster, R. W., Forouhar, A. S., Acevedo-Bolton, G., Fraser, S. E. and Gharib, M. (2003). Intracardiac fluid forces are an essential epigenetic factor for embryonic cardiogenesis. *Nature* **421**, 172-177.

Hurlstone, A. F., Haramis, A. P., Wienholds, E., Begthel, H., Korving, J., Van Eeden, F., Cuppen, E., Zivkovic, D., Plasterk, R. H. and Clevers, H. (2003). The Wnt/beta-catenin pathway regulates cardiac valve formation. *Nature* **425**, 633-637.

Iijima, Y., Nagai, T., Mizukami, M., Matsuura, K., Ogura, T., Wada, H., Toko, H., Akazawa, H., Takano, H., Nakaya, H. et al. (2003). Beating is necessary for transdifferentiation of skeletal muscle-derived cells into cardiomyocytes. *FASEB J.* **17**, 1361-1363.

Koster, R. W. and Fraser, S. E. (2001). Tracing transgene expression in living zebrafish embryos. *Dev. Biol.* **233**, 329-346.

Krug, E. L., Mjaatvedt, C. H. and Markwald, R. R. (1987). Extracellular matrix from embryonic myocardium elicits an early morphogenetic event in cardiac endothelial differentiation. *Dev. Biol.* **120**, 348-355.

Markwald, R. R., Fitzharris, T. P. and Manasek, F. J. (1977). Structural development of Endocardial Cushions. *Am. J. Anat.* **148**, 85-120.

McCue, S., Noria, S. and Langille, B. L. (2004). Shear-induced reorganization of endothelial cell cytoskeleton and adhesion complexes. *Trends Cardiovasc. Med.* **14**, 143-151.

Miyasaka, M. and Tanaka, T. (2004). Lymphocyte trafficking across high endothelial venules: dogmas and enigmas. *Nat. Rev. Immunol.* **4**, 360-370.

Molkentin, J. D., Lu, J. R., Antos, C. L., Markham, B., Richardson, J., Robbins, J., Grant, S. R. and Olson, E. N. (1998). A calcineurin-dependent transcriptional pathway for cardiac hypertrophy. *Cell* **93**, 215-228.

Motoike, T., Loughna, S., Perens, E., Roman, B. L., Liao, W., Chau, T. C., Richardson, C. D., Kawate, T., Kuno, J., Weinstein, B. M., Stainier, D. Y. and Sato, T. N. (2000). Universal GFP reporter for the study of vascular development. *Genesis* **28**, 75-81.

Mumm, J. S. and Kopan, R. (2000). Notch signaling: from the outside in. *Dev. Biol.* **228**, 151-165.

Olson, E. N. (2004). A decade of discoveries in cardiac biology. *Nat. Med.* **10**, 467-474.

Ranger, A. M., Grusby, M. J., Hodge, M. R., Gravallese, E. M., de la Brousse, F. C., Hoey, T., Mickanin, C., Baldwin, H. S. and Glimcher, L. H. (1998). The transcription factor NF-ATc is essential for cardiac valve formation. *Nature* **392**, 186-190.

Runyan, R. B. and Markwald, R. R. (1983). Invasion of mesenchyme into three-dimensional collagen gels: a regional and temporal analysis of interaction in embryonic heart tissue. *Dev. Biol.* **95**, 108-114.

Scheer, N. and Campos-Ortega, J. A. (1999). Use of the Gal4-UAS technique for targeted gene expression in the zebrafish. *Mech. Dev.* **80**, 153-158.

Schott, J. J., Benson, D. W., Basson, C. T., Pease, W., Silberbach, G. M., Moak, J. P., Maron, B. J., Seidman, C. E. and Seidman, J. G. (1998). Congenital heart disease caused by mutations in the transcription factor NKX2-5. *Science* **281**, 108-111.

Sehnert, A. J., Huq, A., Weinstein, B. M., Walker, C., Fishman, M. and Stainier, D. Y. (2002). Cardiac troponin T is essential in sarcomere assembly and cardiac contractility. *Nat. Genet.* **31**, 106-110.

Stainier, D. Y. (2001). Zebrafish genetics and vertebrate heart formation. *Nat. Rev. Genet.* **2**, 39-48.

Stainier, D. Y., Fouquet, B., Chen, J. N., Warren, K. S., Weinstein, B. M., Meiler, S. E., Mohideen, M. A., Neuhauss, S. C., Solnica-Krezel, L., Schier, A. F., Zwartkruis, F., Stemple, D. L., Malicki, J., Driever, W., Fishman, M. C. (1996). Mutations affecting the formation and function of the cardiovascular system in the zebrafish embryo. *Development* **123**, 285-292.

Stainier, D. Y., Beis, D., Jungblut, B. and Bartman, T. (2002). Endocardial cushion formation in zebrafish. *Cold Spring Harb. Symp. Quant. Biol.* **67**, 49-56.

Tallafuss, A. and Bally-Cuif, L. (2003). Tracing of her5 progeny in zebrafish transgenics reveals the dynamics of midbrain-hindbrain neurogenesis and maintenance. *Development* **130**, 4307-4323.

Timmerman, L. A., Grego-Bessa, J., Raya, A., Bertran, E., Perez-Pomares, J. M., Diez, J., Aranda, S., Palomo, S., McCormick, F., Izpisua-Belmonte, J. C. and de la Pompa, J. L. (2004). Notch promotes epithelial-mesenchymal transition during cardiac development and oncogenic transformation. *Genes Dev.* **18**, 99-115.

Trinh, L. A. and Stainier, D. Y. (2004). Fibronectin regulates epithelial organization during myocardial migration in zebrafish. *Dev. Cell* **6**, 371-382.

Trinh, L. A., Yelon, D. and Stainier, D. Y. (2005). Hand2 regulates epithelial formation during myocardial diferentiation. *Curr. Biol.* **15**, 441-446.

Walsh, E. C. and Stainier, D. Y. (2001). UDP-glucose dehydrogenase required for cardiac valve formation in zebrafish. *Science* **293**, 1670-1673.
Webb, S., Brown, N. A. and Anderson, R. H. (1998). Formation of the atrioventricular septal structures in the normal mouse. *Circ. Res.* **82**, 645-656.
Wehman, A. M., Staub, W., Meyers, J. R., Raymond, P. A. and Baier, H. (2005). Genetic dissection of the zebrafish retinal stem-cell compartment. *Dev. Biol.* **281**, 53-65.
Westerfield, M. (2000). *The Zebrafish Book. A Guide for the Laboratory Use of Zebrafish (*Danio rerio*)*, 4th edn, Eugene, OR: University of Oregon Press.
Westin, J. and Lardelli, M. (1997). Three novel Notch genes in zebrafish: implications for vertebrate Notch gene evolution and function. *Dev. Genes Evol.* **207**, 51-63.
Yan, M. and Sinning, A. R. (2001). Retinoic acid administration is associated with changes in the extracellular matrix and cardiac mesenchyme within the endocardial cushion. *Anat. Rec.* **263**, 53-61.
Yelon, D. and Stainier, D. Y. (1999). Patterning during organogenesis: genetic analysis of cardiac chamber formation. *Semin. Cell Dev. Biol.* **10**, 93-98.
Zhou, B., Wu, B., Tompkins, K. L., Boyer, K. L., Grindley, J. C. and Baldwin, H. S. (2005). Characterization of Nfatc1 regulation identifies an enhancer required for gene expression that is specific to pro-valve endocardial cells in the developing heart. *Development* **132**, 1137-1146.

Development

Table S1. Detailed description and allele designation of the mutants identified in our forward genetic screen

Phenotypic group/map position	Allele	Heart defect	Other defects	
Group I: cellular organization defects				
oko meduzy (ome)		s256	Ventricular myocardial defect	RPE defect
-		s251	Disorganized ventricle	Day 2 brain defect
-		s604	Lacks squamous heart cells	
-		s620	Disorganized myocardial myofibrils	
Group II: left-right asymmetry, random heart jogging				
-		s246	Random heart position at 24 hpf	Liver asymmetry
-		s457	Random heart position at 24 hpf	Random endoderm Organ positioning
Group III: large heart				
santa (san)	LG 19	s610	Enlarged heart	
valentine (vtn)	LG 20	s259	Enlarged heart	
Group IV: blood regurgitation at AV canal				
-		s39		
-		s204	Lacks cuboidal AV endocardium	
-		s208		
-	LG 19	s225	AV canal patterning defect	
-		s235		
-		s280		
-	LG 15	s411	Outflow tract stenosis	
		s426		
-	LG 20	s433	AV canal defect	
		s434		
-	LG 19	s619	AV canal defect	
-		s624	Endocardial cushion defect	
Group V: ventricular defects cause sinoatrial regurgitation				
-		s209	Noncontracting ventricle	
		s264		
-		s249	Noncontracting ventricle	
		s271		
-		s213	Noncontracting ventricle	
-		s458	Noncontracting ventricle	
-	LG 14	s275	Ventricle fails at 80 hpf	
-	LG 20	s459	Ventricular defect	Small fins
-		s219	Ventricular defect	
-		s261	Ventricular defect	
-		s272	Ventricular defect	
-		s22	Endocardial hyperplasia	Vascular defects
-		s254	Collapsed ventricle	
		s630		
-		s218	Thin ventricular myocardium	
-		s226	Heart contractility defect	
		s215		
Group VI: sinoatrial regurgitation without obvious ventricular defects				
-		s206	Jaw defect	
-		s224	AV cushion defect	
-		s270	Sinoatrial regurgitation	
-		s274	Sinoatrial regurgitation	
-		s609	Sinoatrial regurgitation	
-		s427	Sinoatrial regurgitation	Thick cardiac ECM
Group VII: heart fins and jaw defects				
hands off	LG 1	s40	Cardia bifida	Fin defect
logelei	LG 9	s201	Ventricular endocardium	Fin and jaw
-	LG 24	s266	Lacks endocardial cushions	Fin and jaw
-		s273	Lacks endocardial cushions	Fin and jaw
-		s245	Collapsed heart	Fin and jaw
Group VIII: day 4 heart defects				
-		s210	AV cushion defect	
-		s211	AV cushion and atrial endocardium	
-		s247	AV cushion and atrial endocardium	
-		s252	Collapsed cardiac lumen	
-		s606	Heart defect	Jaw defect
-		s612	Endocardial cushion defect	Circulation defect
		s277		

Mutants are ordered in phenotypic groups according to their AV canal phenotype. Additional phenotypes described here are observed at 55 and/or 120 hpf by bright-field microscopy. Map information is indicated when available.